SPANDIDOS PUBLICATIONS

ONCOLOGY LETTERS 17: 4024-4033, 2019

Enhanced targeting of prostate cancer-initiating cells by salinomycin-encapsulated lipid-PLGA nanoparticles linked with CD44 antibodies

JUN WEI[1], JIN SUN[2] and YU LIU[1]

[1]Department of Urology, Hanyang Hospital Affiliated to Wuhan University of Science and Technology, Wuhan, Hubei 430050; [2]Department of Pharmacy, The Naval Military Medical University, Shanghai 200433, P.R. China

Received March 29, 2018; Accepted December 17, 2018

DOI: 10.3892/ol.2019.10050

Abstract. Prostate cancer is the fifth most common cause of cancer-associated mortality in males worldwide. The survival of prostate cancer-initiating cells (CICs) is an important factor behind the metastasis and recurrence of prostate cancer. The cluster of differentiation (CD) 44 antigen is considered an important marker for prostate CICs. Salinomycin is a potent therapeutic drug against CICs. The present study demonstrated that salinomycin exerts potent activity against $CD44^+$ prostate CICs. To further enhance this anticancer effect, salinomycin-encapsulated lipid-poly(lactic-co-glycolic acid) nanoparticles linked with CD44 antibodies (SM-LPN-CD44) were generated. The anticancer effect of the nanoparticles was investigated in a series of assays, including a cytotoxicity assay, flow cytometry and anticancer assay in prostate cancer-bearing mice *in vivo*. The results revealed that SM-LPN-CD44 could efficiently and specifically promote the delivery of salinomycin to $CD44^+$ prostate CICs, and there by achieve greater inhibition of the cells compared with that achieved by salinomycin and non-targeted nanoparticles. To the best of our knowledge, this is the first study to report improved therapeutic effects against prostate CICs achieved by the enhancement of targeted drug delivery via nanoparticles conjugated with CD44 antibodies. Therefore, SM-LPN-CD44 nanoparticle-based therapy represents a novel approach to eliminate prostate CICs and is a promising potential treatment strategy for prostate cancer.

Introduction

Cancer of the prostate, a gland in the male genital system, is a growing concern in the field of global epidemiology. Statistics for the USA demonstrate that ~20% of males will be diagnosed with prostate cancer during their lifetime (1). Prostate cancer contributes significantly to the mortality of men and ranks as the fifth most common cause of cancer-associated mortality among men in the USA (1). Every year, >1,000,000 cases are diagnosed and >300,000 individuals succumb to the disease worldwide (2). Therefore, there is an urgent requirement for alternative therapeutic strategies to improve prostate cancer prognosis.

Although improvements have been made in the field of prostate cancer therapy, therapy failure and low survival rates persist among patients. This can be attributed to metastasis, drug resistance and high rates of recurrence (3,4). One of the main causes for these phenomena is the persistence of prostate cancer-initiating cells (CICs) (5-7). Therefore, the elimination of prostate CICs may contribute significantly towards treatment strategies for prostate cancer. Cluster of differentiation (CD) 44, a multi-functional protein associated with cell adhesion and signaling, is one of the major markers for prostate CICs (8,9). Patrawala *et al* (9) demonstrated that compared with $CD44^-$ prostate cancer cells, $CD44^+$ cells are more aggressive, as is reflected by their higher clonogenicity, tumorigenicity and metastatic ability. Furthermore, certain intrinsic characteristics of progenitor cells have been identified in $CD44^+$ prostate CICs; this includes increased expression of a group of stemness genes, including β-catenin and octamer-binding transcription factor 3/4 (9). Therefore, the eradication of $CD44^+$ prostate CICs may enhance therapeutic efficacy in the treatment of prostate cancer.

Salinomycin, an antibiotic isolated from *Streptomyces albus*, is a therapeutic drug with potent activity against CICs in various types of cancer (10-13). The mechanisms of action of this drug include the inhibition of the Wnt pathway and the induction of apoptosis (12). A number of studies have reported that salinomycin can exert potent anticancer effects in prostate cancer cells via these mechanisms (14-16). However, to the best of our knowledge, only one study has confirmed the superior therapeutic effects of salinomycin against prostate CICs (13). Therefore, more data is required to support claims that salinomycin exhibits high therapeutic efficacy against prostate CICs.

Despite its promise as an anticancer agent, the aqueous solubility of salinomycin is poor, resulting in low bioavailability

Correspondence to: Dr Yu Liu, Department of Urology, Hanyang Hospital Affiliated to Wuhan University of Science and Technology, 53 Moshuihu Road, Wuhan, Hubei 430050, P.R. China
E-mail: 286737962@qq.com

Key words: prostate cancer, cancer-initiating cells, nanoparticles, cluster of differentiation 44, antibody

and poor therapeutic efficacy *in vivo* (10,11,17). A possible solution to this problem involves nanoparticle-based strategies. Nanoparticles have been demonstrated to markedly improve the solubility and therapeutic index of poorly soluble drugs by their controlled and targeted delivery (6,7). With this in mind, numerous studies have developed salinomycin-loaded nanoparticles to facilitate the preclinical investigation of this drug as a cancer therapeutic strategy (10,11,17).

Lipid-polymer hybrid nanoparticles consisting of biodegradable polymers and lipids represent superior candidate drug delivery systems, as they combine the advantages of liposomes and polymer nanoparticles (18,19). Liposomes are characterized by superior biocompatibility and are attractive due to the ease with which modifications can be made to their component hydrophilic polymer, polyethylene glycol (PEG), or their targeting molecules, including antibodies, peptides and aptamers (20). The advantages of polymer nanoparticles, including poly(lactide-co-glycolide acid) (PLGA), which is the most commonly used, include controlled and sustained release, high drug loading capacity and superior stability (21,22). Therefore, the advantages of lipid-polymer hybrid nanoparticles include superior biocompatibility, ease of modification, controlled and sustained release, stability and high drug loading capacity (18,19).

There is currently considerable interest in antibody-targeted nanoparticles as a strategy to promote chemotherapeutic efficiency by ensuring targeted delivery of therapeutic drugs, and this approach has been demonstrated to be successful in the treatment of several types of cancer (23,24). Since CD44 is a marker for prostate CICs, it may be possible to use the CD44 antibody to promote the targeted delivery of salinomycin-loaded nanoparticles to CICs.

In order to accomplish this, the current study generated salinomycin-encapsulated lipid-PLGA nanoparticles linked with CD44 antibodies (SM-LPN-CD44). The characteristics of SM-LPN-CD44 were then investigated to evaluate its targeting ability and its therapeutic effect against prostate CICs.

Materials and methods

Reagents and cell culture. PLGA (50:50 molar ratio between lactide and glycolide; 40-75 kDa), polyvinyl alcohol (PVA; 30-70 kDa), 2-iminothiolane, salinomycin and organic reagents were all purchased from Sigma-Aldrich; Merck KGaA (Darmstadt, Germany). The lipids, including 1,2-distearoyl-*sn*-glycero-3-phosphoethanolamine-N-[maleimide (PEG)-2000] (DSPE-PEG-Mal), 1,2-dioleoyl-*sn*-glycero-3-phosphoethanolamine-N-(carboxyfluorescein) (PECF), phosphatidylcholine and cholesterol were obtained from Avanti Polar Lipids (Alabaster, AL, USA). R&D Systems, Inc., (Minneapolis, MN, USA) provided the rat anti-human CD44 Alexa Fluor® 488-conjugated antibody (cat. no. FAB6127G) and recombinant rat anti-human CD44 monoclonal antibody (cat. no. MAB6127). The CD44 Fab' from the recombinant rat anti-human CD44 monoclonal antibody was isolated using a protocol described in a previous study (16). The Pierce bicinchoninic acid (BCA) protein assay kit, RPMI 1640 medium, Dulbecco's modified Eagle's medium (DMEM), DMEM/Ham's F-12 (DMEM/F12) medium, fetal bovine serum (FBS), B27, epidermal growth factor (EGF), basic fibroblast growth factor (bFGF) and insulin-transferrin-selenium (ITS) were purchased from Thermo Fisher Scientific Inc. (Waltham, MA, USA). The CD44 MicroBead kit was obtained from Miltenyi Biotec GmbH (Bergisch Gladbach, Germany).

The DU145 cell line, a human prostate cancer cell line derived from a metastatic site, and the 22RV1 cell line, a human prostate carcinoma epithelial cell line, were obtained from the American Type Culture Collection (Manassas, VA, USA). The cultures were maintained in DMEM supplemented with 10% FBS, 100 U/ml penicillin and 100 μg/ml streptomycin, at 37˚C in a humidified incubator with 5% CO_2.

CD44 expression in prostate cancer cell lines. Flow cytometry was performed to analyze the expression of CD44 in the two prostate cancer cell lines. The cultured cells were dissociated into a single cell suspension, which was then incubated with rat anti-human CD44 Alexa Fluor® 488-conjugated antibody diluted in 1% fetal bovine serum (1:500 dilution; FBS used as a blocking reagent, Thermo Fisher Scientific, Inc.) at 1 μg/ml for 30 min at 4˚C. Subsequently, the cells were washed with PBS to remove unconjugated antibody and resuspended in PBS. The FACSCalibur flow cytometer (Becton, Dickinson and Company, Franklin Lakes, NJ, USA) was used to determine the proportion of positively stained cells. Expression was analyzed using FlowJo, version 10 (FlowJo LLC, Ashland, OR, USA).

Magnetic cell sorting-based separation of CD44$^+$ cells. The separation of CD44$^+$ cells was performed using the CD44 MicroBead kit according to the manufacturer's protocol. The final proportion of positively stained cells was determined by flow cytometry.

Evaluation of the tumorsphere formation ability of cells. The formation of tumorspheres when single cells are suspended in serum-free medium indicates the self-renewal ability of CICs (25-27). Briefly, prostate cancer cells were suspended in stem cell medium in Corning® ultra-low adherent 6-well dishes (Corning Inc., Corning, NY, USA) at a density of $5x10^3$ cells/well. The composition of the stem cell medium was as follows: DMEM/F12 supplemented with B27 (1x), ITS (1x), EGF (20 ng/ml) and bFGF (20 ng/ml). The cells were cultured for 7 days, following which the number of tumorspheres was counted using light microscopy (magnification, x50). The tumorsphere formation rate of the untreated group was used as a control, in which the rate was defined as 100%. To obtain a second passage, the first passage tumorspheres were washed with PBS, disaggregated using cell dissociation reagent (StemPro® Accutase®; Thermo Fisher Scientific, Inc.) and propagated in stem cell medium for 7 days.

In vivo investigation of tumorigenicity. The tumorigenicity of prostate cancer cells *in vivo* was studied in BALB/c nude mice (4-5 weeks old; male; ~20 g; 24 mice were used, 6 mice/group) purchased from the Shanghai Experimental Animal Center (Shanghai, China). The mice were acclimated for ~7 days in a pathogen-free environment. Animals were housed in separate cages (3-4 animals per cage) maintained under a controlled atmosphere (humidity of 50±7% and a temperature of 21±1˚C)

and with a 12:12 h light/dark cycle. The mice were allowed free access to food and water. All animal procedures were approved by the Animal Administrative Committee of the Naval Medical University (Shanghai, China) and performed in accordance with their guidelines. Briefly, varying numbers of $CD44^+$ or $CD44^-$ prostate cancer cells (range, $2x10^3$-$1x10^6$ cells) were isolated from the cell lines using the aforementioned magnetic cell-sorting method. The collected cells were mixed with BD Matrigel™ (Becton, Dickinson and Company) and the mixture was injected subcutaneously into the right flank of the mice. Subsequent tumor formation was observed and recorded for a period of 15 weeks. Mice were sacrificed if the tumor size exceeded 1,500 mm^3.

Preparation of lipid-PLGA hybrid nanoparticles. Lipid-PLGA hybrid nanoparticles were generated using the emulsion-solvent evaporation-based procedure. In brief, 0.5 mg salinomycin and 5 mg PLGA were completely dissolved in acetone to form the oil phase. The oil solution was injected into 2% PVA solution, followed by homogenization. The mini-emulsion was then poured into a 0.2% PVA solution and mixed rapidly for 6 h to remove any remaining acetone by evaporation. The nanoparticles were recovered by ultracentrifugation (80,000 x g) at 25˚C for 30 min. At the same time, a lipid film composed of phosphatidylcholine (Avanti Polar Lipids), DSPE-PEG-Mal and cholesterol (57:3:40 molar ratio) was formed in a round-bottomed flask upon using a vacuum rotary evaporator. Once the lipid film was formed, the recovered nanoparticles were added to hydrate it. A hand-held extruder (Avanti Polar Lipids) with 200-nm membranes was used to extrude the lipid-polymer suspension in order to create small and homogeneous nanoparticles. The resultant lipid-polymer nanoparticles were washed with distilled water by ultracentrifugation in Amicon® Ultra-4 centrifugal filter devices (nominal molecular weight limit, 100,000; EMD Millipore, Billerica, MA, USA). Furthermore, CD44 Fab' was thiolated by the addition of 2-iminothiolane (molar ratio of 1:100) (16). Thiolated CD44 Fab' was incubated with the nanoparticles (molar ratio of 1:10) for 6 h at room temperature in order to conjugate thiolated antibodies with the nanoparticles. The Amicon centrifugal filters were used to remove unconjugated Fab'. Non-targeted nanoparticles were developed using a similar protocol, but with the exclusion of Fab'. Blank nanoparticles were developed using a similar protocol, but with the exclusion of salinomycin and Fab'. The fluorescent PECF-labeled nanoparticles were constructed using a similar protocol except that 0.1% PECF was included as part of the lipid film composition. The following abbreviations are used to describe the nanoparticles used in the present study: SM-LPN, salinomycin-encapsulated lipid-PLGA nanoparticles; SM-LPN-CD44, salinomycin-encapsulated lipid-PLGA nanoparticles linked with CD44 antibodies; and LPN-CD44, blank lipid-PLGA nanoparticles linked with CD44 antibodies.

Conjugation efficacy of antibodies with nanoparticles. Ultrafiltration of the nanoparticles was performed to evaluate the conjugation efficacy of antibodies with nanoparticles. Briefly, the antibodies were incubated with the nanoparticles and the mixture was centrifuged in Amicon centrifugal filters (molecular weight cut-off value, 100 kDa) to exclude unconjugated antibodies. The unconjugated antibodies removed were measured using the Pierce BCA protein assay kit. The efficacy of conjugation between antibodies and the fabricated nanoparticles were evaluated using the following equation: $(M_t-M_u)/M_t$, where M_t denotes the total mass of added antibodies and M_U represents the mass of unconjugated antibodies.

Size, ζ potential, morphology and drug loading capacity of lipid-PLGA nanoparticles. A lipid-PLGA solution, prepared by diluting 100 µl nanoparticles in 1.9 ml distilled water, was run through a Zetasizer Nano ZS90 (Malvern Instruments, Ltd., Malvern, UK) to evaluate the nanoparticle size and ζ potential. The salinomycin encapsulation efficiency and loading capacity of the lipid-PLGA nanoparticles was determined by reverse-phase high-performance liquid chromatography (HPLC) using the universal reverse phase Diamonsil® C-18 column (size of packing carriers, 5 µm; length x width, 250x4.5 mm; Dikma Technologies Inc., Lake Forest, CA, USA). Briefly, 1 ml dichloromethane was added to 2 mg lyophilized nanoparticles to dissolve them. The dichloromethane was removed completely by evaporation via vacuum drying, and methanol was added to dissolve the residual nanoparticles by thorough vortexing. The analysis was performed using the L-2000 HPLC system (Hitachi, Ltd., Tokyo, Japan). The mobile phase used was water/tetrahydrofuran/acetonitrile/phosphoric acid (v/v/v/v, 10/4/86/0.01) and the flow rate was 1 ml/min. The detection wavelength for salinomycin was set at 210 nm. Finally, a PECF calibration curve was used to evaluate the drug loading capacity of the labeled nanoparticles.

Salinomycin release profile of encapsulated lipid-PLGA nanoparticles. Lipid-PLGA nanoparticles (0.5 mg/ml) were suspended in PBS or PBS supplemented with 10% FBS in a centrifuge tube. Subsequently, the nanoparticles were placed on an orbital shaker moving at 100 rpm at a temperature of 37˚C. At multiple designated time points (0.5, 1, 2, 3, 4, 6, 8, 12, 24, 48, 72 and 148 h) during the 150 h drug release period, the tubes were centrifuged (12,000 x g for 30 min) and the supernatant was evaluated by reverse-HPLC, as aforementioned. The cumulative salinomcyin release rate of the nanoparticles was calculated using the following formula: (M_i/M_t) x 100, where M_i is the mass of cumulative released salinomycin and M_t is the total mass of salinomycin used to encapsulate the nanoparticles.

In vitro targeting of fluorescent nanoparticles to prostate cancer cells. Flow cytometry was used to study the *in vitro* targeting of fluorescent nanoparticles as described previously (10). Briefly, prostate cancer cells were seeded in a 12-well cell culture plate at a density of $5x10^5$ cells per well, and incubated overnight at 37˚C. The old medium was replaced with fresh medium in which PECF-loaded nanoparticles (1 µg/ml PECF) were dissolved. The cells were incubated for a further 2 h. The cells were then washed three times with PBS to remove unbound nanoparticles and trypsinized. The cells were subsequently resuspended in PBS and analyzed using the FACSCalibur flow cytometer.

Table I. Examination characteristics of nanoparticles.

Nanoparticle	Size, nm	ζ potential, mv	PDI	Drug loading, %	EE, %
SM-LPN	125.6±15.1	-13.4±5.9	0.13±0.05	8.1±3.7	76.3±9.1
SM-LPN-CD44	139.9±18.5	-17.3±4.4	0.17±0.06	8.9±2.6	74.2±8.7
LPN-CD44	131.1±16.7	-15.8±6.1	0.14±0.07	-	

Data are presented as the mean±standard deviation (n=4). PDI, polydispersity index; EE, encapsulation efficacy; SM-LPN, salinomycin-encapsulated lipid-poly(lactide-co-glycolide acid) nanoparticles; SM-LPN-CD44, salinomycin-encapsulated lipid-poly(lactide-co-glycolide acid) nanoparticles linked with CD44 antibodies; LPN-CD44, blank lipid-poly(lactide-co-glycolide acid) nanoparticles linked with CD44 antibodies; CD, cluster of differentiation.

Evaluation of cytotoxicity of nanoparticles towards prostate cancer cell lines. The cytotoxicity of nanoparticles against the prostate cancer cell lines was evaluated with the CCK-8 assay kit (Dojindo Molecular Technologies, Inc., Kumamoto, Japan), according to the manufacturer's protocol (10). Briefly, the cells were washed, trypsinized, seeded in 96-well cell culture plates at a density of $3x10^3$ cells/well and cultured overnight. Spent medium was discarded and replaced with fresh medium containing free salinomycin or salinomycin PLGA-lipid nanoparticles at various concentrations (0.01, 0.04, 0.12, 0.37, 1.11, 3.33, 10.00, 30.00, 90.00 and 270.00 μg/ml). Following incubation for 72 h at 37˚C, the medium was replaced with fresh medium containing no drug. The viability of the treated cells was determined by performing a CCK-8 assay using a microplate reader. The data was analyzed using GraphPad Prism version 5 (GraphPad Software, Inc., La Jolla, CA, USA) to calculate the final half maximal inhibitory concentration (IC_{50}) values.

Evaluation of the impact of nanoparticles on the proportion of CICs in cultured cells. Tumorsphere formation and the proportion of $CD44^+$ cells were taken as parameters for evaluation of the impact of the generated nanoparticles on the proportion of CICs in the cultured cells. In brief, cells were washed, trypsinized and seeded at a density of $5x10^4$ cells/well in 12-well cell culture plates. Following incubation overnight, the cells were washed with PBS and treated with fresh medium containing dissolved nanoparticles (an amount equivalent to 5 μg/ml salinomycin). Following 24 h of incubation, the spent medium was aspirated and fresh medium with no nanoparticles was added. Following a further 72 h incubation, the cells were washed, trypsinized and propagated to evaluate the formation of tumorspheres. Alternatively, flow cytometry was performed to measure the percentage of $CD44^+$ cells from trypsinized cells.

Statistical analysis. The data were analyzed using SPSS (version 13; SPSS, Inc., Chicago, IL, USA). Two groups were statistically compared using the Student's non-paired t-test. Three or more groups were compared using one-way analysis of variance followed by the Student-Newman-Keuls or Dunnett's post hoc tests. $P<0.05$ was considered to indicate a statistically significant difference. All data are expressed as the mean ± standard deviation.

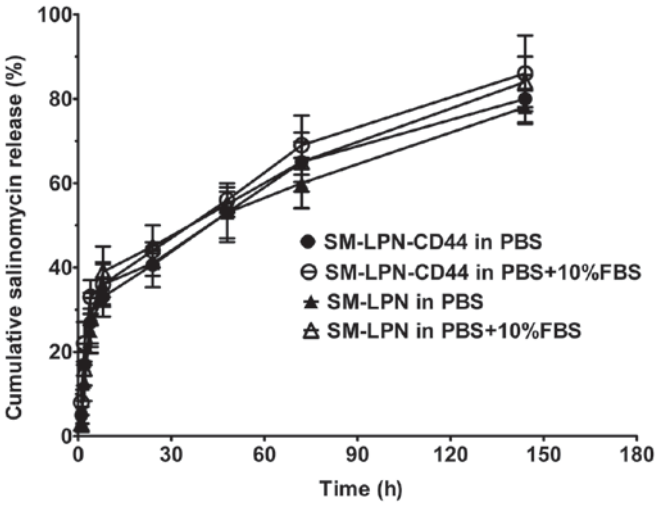

Figure 1. Salinomycin release from nanoparticles. The release media were PBS and PBS with 10% FBS. The accumulated salinomycin release rate of the nanoparticles was measured using the following formula: (M_i/M_t) x 100, where M_i is the mass of accumulated released salinomycin and M_t is the total amount of salinomycin. Data are presented as the mean ± standard deviation (n=3). SM-LPN-CD44, salinomycin-encapsulated lipid-poly (lactide-co-glycolide acid) nanoparticles linked with CD44 antibodies; SM-LPN, salinomycin-encapsulated lipid-poly(lactide-co-glycolide acid) nanoparticles; FBS, fetal bovine serum.

Results

Characteristics of generated lipid-PLGA hybrid nanoparticles. The lipid-PLGA nanoparticles were generated by following three simple steps. Firstly, the PLGA nanoparticle core was prepared by the emulsion-solvent evaporation procedure. Secondly, the core was coated with the lipid shell by lipid-film based hydration. Next, the thiolated antibodies were linked to the nanoparticles by a reaction between sulfhydryl and maleimide groups. The size, ζ potential and drug loading capacity of the nanoparticles are presented in Table I. SM-LPN, the unconjugated nanoparticles, had a size of 125.6 nm. Nanoparticles conjugated with antibodies were larger; SM-LPN-CD44 and LPN-CD44 had a size of 139.9 and 31.1 nm, respectively. The ζ potential of all the nanoparticles was negative and ~-15 mV. The drug loading capacity of all nanoparticles was ~8% and they all exhibited an encapsulation efficiency of ~75%. The conjugation efficiency of antibodies on SM-LPN-CD44 was ~12%. As demonstrated in Fig. 1, the

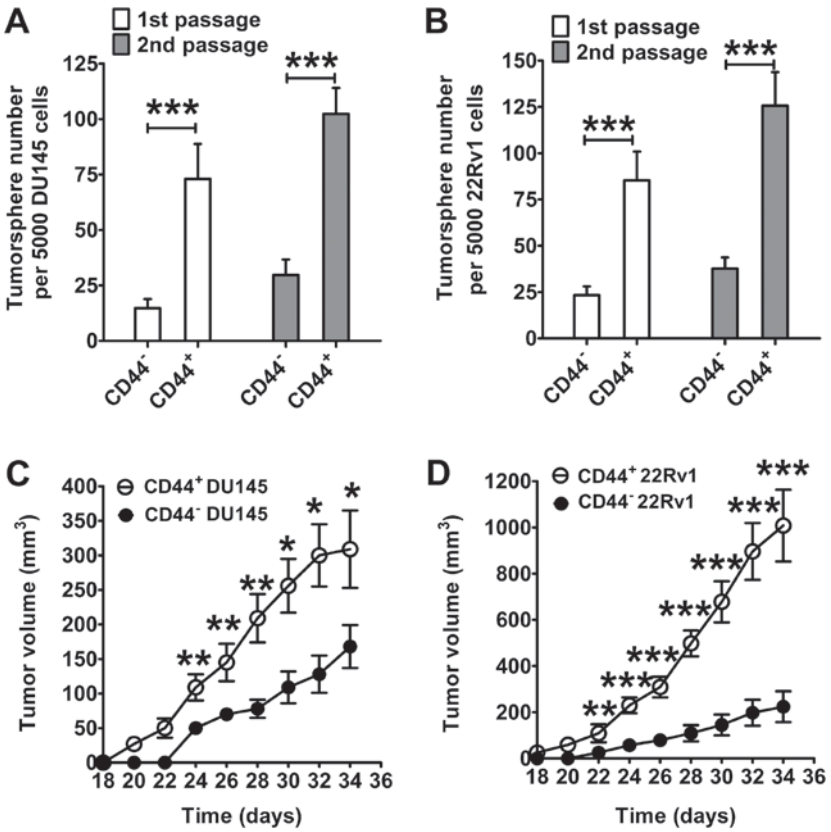

Figure 2. CD44+ prostate cancer cells exhibit the properties of prostate cancer-initiating cells, as demonstrated by tumorsphere formation and tumor growth in nude mice. Tumorsphere formation in serum-free medium of (A) DU145 and (B) 22RV1 prostate cancer cells. Growth curves of prostate cancer in nude mice following injection with $2x10^5$ (C) DU145 or (D) 22RV1 prostate cancer cells. Data are presented as the mean ± standard deviation (n=6). *P<0.05, **P<0.01, ***P<0.001. CD, cluster of differentiation.

salinomycin release assay indicated that all the nanoparticles exhibited a burst release, with ~45% of salinomycin released within the first 24 h. Following 120 h, the cumulative salinomycin released gradually reached 80%, suggesting that all the nanoparticles exhibit a sustained drug release for 120 h following the initial 24 h period. The salinomycin release profile of the nanoparticles in PBS was not significantly different from their release profile in PBS supplemented with 10% FBS (P>0.05).

CD44+ prostate cancer cells exhibit properties of CICs. CD44 MicroBead Kit-based cell sorting was used to isolate CD44+ cells from prostate cancer cells. A high percentage (>98%) of CD44+ cells were obtained from the original cell mixture, in which the percentage of CD44+ cells was 20-35% (data not shown). A tumorsphere formation assay was used to identify CICs. As presented in Fig. 2A, CD44+ DU145 cells generated a significantly higher number of tumorspheres compared with the CD44- DU145 cells (first passage, P<0.001; second passage, P<0.001). Similar results were obtained in 22RV1 cells (first passage, P<0.001; second passage, P<0.001; Fig. 2B). Furthermore, CD44+ cells demonstrated an enhanced capacity for promoting prostate cancer formation in nude mice compared with CD44- cells (Fig. 2C and D). Compared with tumors formed from CD44- cells, the mean volume of CD44+ cell-initiated tumors was significantly higher from day 24 onward for DU145 cells, and from day 22 onward for 22RV1 cells (P<0.05). At the endpoint (day 34), the mean volume of CD44+ DU145 cell-initiated tumors was 309 mm^3, which was significantly larger than the mean volume of CD44- DU145 cell-initiated tumors (168 mm^3) (P<0.001; Fig. 2C). Fig. 2D presents similar results in 22RV1 cells. On day 34, the mean volume of tumors initiated by CD44+ 22RV1 cells was 1,008 mm^3, which was significantly larger than the mean volume of tumors initiated by CD44- 22RV1 cells (224 mm^3; P<0.001).

Subsequently, the tumorigenicity of various numbers of prostate cancer cells introduced into mice was evaluated (Table II). Notably, a 100% incidence rate of tumors (9/9) was identified in mice injected with CD44+ DU145 cells at a concentration ≥$1x10^4$ cells. By contrast, only a 55% incidence rate of tumors (5/9) was observed in mice injected with $1x10^6$ CD44- DU145 cells, indicating that CD44+ DU145 cells exhibit a significantly greater tumorigenic potential compared with CD44- DU145 cells. Similarly, CD44+ 22RV1 cells demonstrated significantly greater tumorigenic potential compared with CD44- 22RV1 cells. A 100% incidence rate of tumors (9/9) was identified in mice injected with CD44+ 22RV1 cells at a concentration of ≥$1x10^4$ cells. By contrast, only a 78% incidence rate of tumors (7/9) was observed in mice injected with $1x10^6$ CD44- 22RV1 cells, indicating that CD44+ 22RV1 cells exhibit significantly greater tumorigenic potential compared with CD44- 22RV1 cells. Based on the aforementioned results, it may be concluded that the tumorigenicity of CD44+ prostate cancer cells was significantly higher compared with that of

Table II. *In vivo* tumorigenicity of prostate cancer cells in mice.

	Number of cells					
Cell type	$1x10^6$	$1x10^5$	$5x10^4$	$1x10^4$	$5x10^3$	$2x10^3$
$CD44^-$ DU145	5/9	3/9	1/9	0/9	0/9	0/9
$CD44^+$ DU145	9/9	9/9	9/9	9/9	8/9	5/9
$CD44^-$ 22RV1	7/9	6/9	3/9	1/9	0/9	0/9
$CD44^+$ 22RV1	9/9	9/9	9/9	9/9	7/9	4/9

CD, cluster of differentiation.

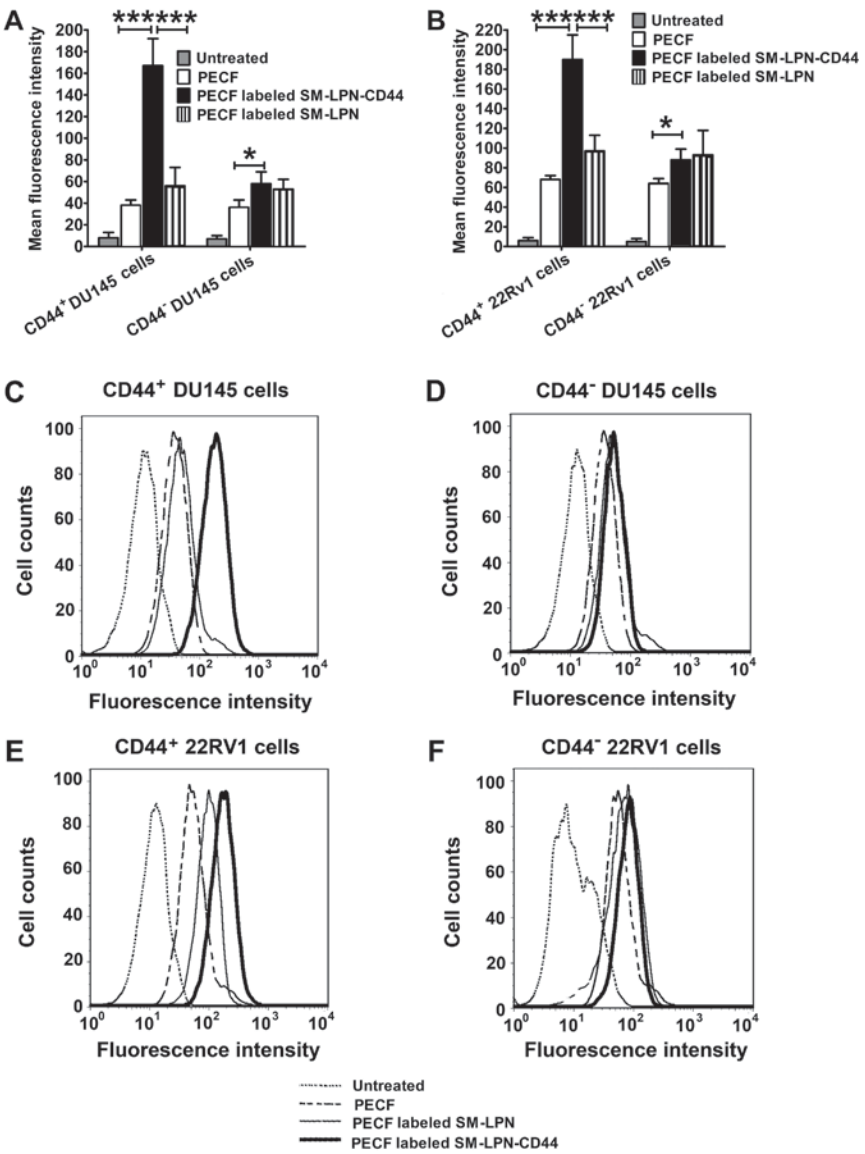

Figure 3. *In vitro* targeting of fluorescent probe-labeled nanoparticles in prostate cancer cells. Fluorescence intensity in (A) DU145 cells and (B) 22RV1 cells. Arbitrary units of fluorescence were used to assess fluorescence intensity. The differences among groups were evaluated by one-way analysis of variance followed by Newman-Keuls post hoc test. Data are presented as the mean ± standard deviation (n=3). $^*P<0.05$ and $^{***}P<0.001$. (C-F) Representative flow cytometry histograms. PECF, 1,2-dioleoyl-*sn*-glycero-3-phosphoethanolamine-N-(carboxyfluorescein); SM-LPN-CD44, salinomycin-encapsulated lipid-poly(lactide-co-glycolide acid) nanoparticles linked with CD44 antibodies; SM-LPN, salinomycin-encapsulated lipid-poly(lactide-co-glycolide acid) nanoparticles; CD, cluster of differentiation.

$CD44^-$ prostate cancer cells, indicating that $CD44^+$ cells possess the features of prostate CICs.

Fluorescently labeled CD44 antibody-conjugated nanoparticles demonstrate highly specific targeting to $CD44^+$

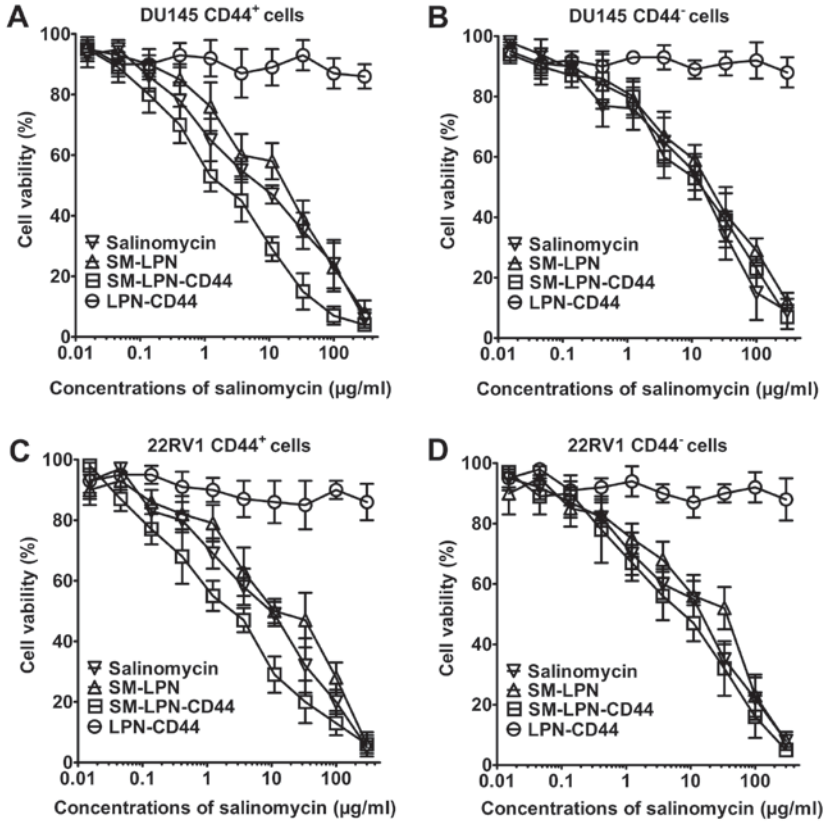

Figure 4. Cytotoxicity of nanoparticles examined in prostate cancer cells using the Cell Counting Kit-8 assay. Cell viability in (A) DU145 $CD44^+$ cells, (B) DU145 $CD44^-$ cells, (C) 22RV1 $CD44^+$ cells and (D) 22RV1 $CD44^-$ cells. Data are presented as the mean ± standard deviation (n=3). SM-LPN-CD44, salinomycin-encapsulated lipid-poly(lactide-co-glycolide acid) nanoparticles linked with CD44 antibodies; SM-LPN, salinomycin-encapsulated lipid-poly(lactide-co-glycolide acid) nanoparticles; LPN-CD44, blank lipid-poly(lactide-co-glycolide acid) nanoparticles linked with CD44 antibodies; CD, cluster of differentiation.

prostate cancer cells in vitro. As a common green fluorescent tracer, PECF was used to evaluate the *in vitro* targeting of fluorescent nanoparticles to cancer cells (Fig. 3). As demonstrated in Fig. 3A, C and D, the uptake of PECF-labeled SM-LPN-CD44 in $CD44^+$ DU145 cells was significantly higher compared with that of PECF labeled SM-LPN and free PECF ($P<0.001$). PECF-labeled SM-LPN-CD44 demonstrated a similar uptake rate to that of PECF-labeled SM-LPN in $CD44^-$ DU145 cells, but exhibited a significantly higher uptake rate compared with free PECF ($P<0.05$). In 22RV1 cells, similar results were obtained (Fig. 3B, E and F). PECF-labeled SM-LPN-CD44 exhibited a significantly greater uptake rate compared with PECF-labeled SM-LPN and free PECF in $CD44^+$ 22RV1 cells ($P<0.001$), whereas it demonstrated a similar uptake rate compared with PECF-labeled SM-LPN in $CD44^-$ 22RV1 cells.

Nanoparticles demonstrate no significant cytotoxicity, whereas salinomycin exhibits dose-dependent cytotoxicity against prostate cancer cells. As demonstrated in Fig. 4, LPN-CD44 exhibited no significant cytotoxicity against prostate cancer cells. By contrast, dose-dependent cytotoxicity was induced by salinomycin, SMP-LPN and SM-LPN-CD44, as can be observed from their respective inverse sigmoid dose-dependent curves. The IC_{50} values of the drugs are presented in Table III. In $CD44^+$ DU145 cells, SM-LPN demonstrated cytotoxicity similar to that of free salinomycin (IC_{50}, 8.6 vs. 5.3 μg/ml, respectively). Compared with SM-LPN and salinomycin, SM-LPN-CD44 exhibited significantly increased cytotoxicity (IC_{50}, 1.4 μg/ml; $P<0.05$). By contrast, no significant difference was identified in the IC_{50} values for SM-LPN-CD44 (16.3 μg/ml), SM-LNP (18.1 μg/ml) and salinomycin (15.0 μg/ml) in $CD44^-$ DU145 cells. Similar results were observed in $CD44^+$ 22RV1 cells, with SM-LPN-CD44 cytotoxicity (2.4 μg/ml) revealed to be significantly higher compared with that of SM-LNP (10.9 μg/ml) and salinomycin (7.7 μg/ml) ($P<0.05$). By contrast, no significant differences were observed in the cytotoxicity of SM-LPN-CD44 (20.8 μg/ml) compared with SM-LPN (23.4 μg/ml) and salinomycin (17.7 μg/ml) in $CD44^-$ 22RV1 cells. It was concluded that SM-LPN-CD44 demonstrates preferential cytotoxicity against $CD44^+$ prostate cancer cells.

A proportion of CICs is reduced in prostate cancer cell cultures treated with SM-LPN-CD44. Fig. 5 demonstrates the impact of nanoparticles on the proportion of CICs in cultured prostate cancer cells. In DU145 cells, treatment with salinomycin significantly reduced the number of tumorspheres propagated from passaged cells ($P<0.01$; Fig. 5A). The inhibitory capacity of SM-LPN was similar to that of salinomycin. However, the number of tumorspheres observed following SM-LPN-CD44 treatment was further reduced when compared with the number following salinomycin or SM-LPN treatment ($P<0.05$). Treatment with LPN-CD44 exhibited no significant effect on the number of tumorspheres. Furthermore, in 22RV1 cells, SM-LPN-CD44 was the most effective inhibitor of

Table III. IC_{50} values of salinomycin and nanoparticles in prostate cancer cells at 72 h.

	IC_{50}, μg/ml			
Treatment	$CD44^+$ DU145	$CD44^-$ DU145	$CD44^+$ 22RV1	$CD44^-$ 22RV1
Salinomycin	5.3±2.3	15.9±7.6	7.7±5.3	17.7±5.4
SM-LPN	8.6±4.9	18.1±7.3	10.9±5.7	23.4±6.5
SM-LPN-CD44	1.4±1.3	19.3±6.8	2.4±1.6	20.8±6.9
LPN-CD44	>300.0	>300.0	>300.0	>300.0

Data are presented as mean ± standard deviation (n=3). SM-LPN, salinomycin-encapsulated lipid-poly(lactide-co-glycolide acid) nanoparticles; SM-LPN-CD44, salinomycin-encapsulated lipid-poly(lactide-co-glycolide acid) nanoparticles linked with CD44 antibodies; LPN-CD44, blank lipid-poly(lactide-co-glycolide acid) nanoparticles linked with CD44 antibodies; CD, cluster of differentiation; IC_{50}, half maximal inhibitory concentration.

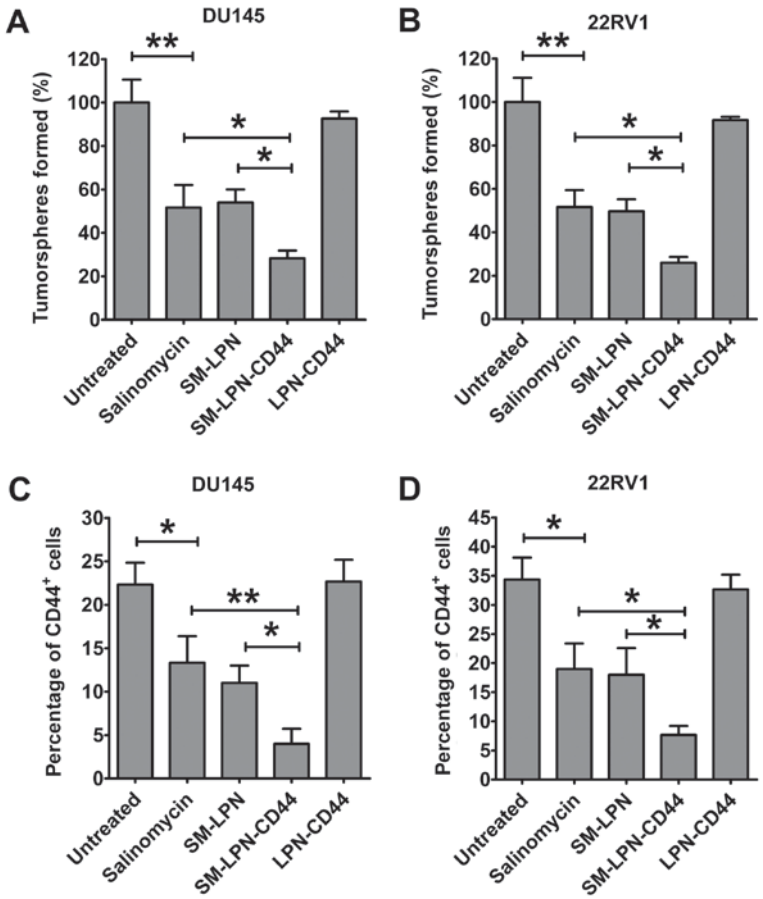

Figure 5. Impact of nanoparticles on the proportion of cancer-initiating cells in prostate cancer cells. Evaluation of tumorsphere formation in (A) DU145 and (B) 22RV1 cells following the treatment of prostate cancer cells and culture in serum-free medium. The percentage of $CD44^+$ cells in (C) DU145 and (D) 22RV1 cells was evaluated by flow cytometry following treatment of prostate cancer cells. Data are presented as the mean ± standard deviation (n=3). $^*P<0.05$ and $^{**}P<0.01$. SM-LPN-CD44, salinomycin-encapsulated lipid-poly(lactide-co-glycolide acid) nanoparticles linked with CD44 antibodies; SM-LPN, salinomycin-encapsulated lipid-poly(lactide-co-glycolide acid) nanoparticles; LPN-CD44, blank lipid-poly(lactide-co-glycolide acid) nanoparticles linked with CD44 antibodies.

tumorsphere formation, whereas treatment with LPN-CD44 exhibited no significant effect (Fig. 5B).

Consistent with the aforementioned results, it was identified that the percentage of $CD44^+$ DU145 cells was significantly reduced following salinomycin treatment ($P<0.05$; Fig. 5C). Salinomycin and SM-LPN each demonstrated a degree of inhibition that was similar to their inhibition of tumorsphere propagation. Furthermore, the percentage of $CD44^+$ DU145 cells following treatment with SM-LPN-CD44 was the lowest among all experimental groups. Similar results were obtained in 22RV1 cells (Fig. 5D). Therefore, SM-LPN-CD44 was confirmed to exhibit the highest efficiency in inhibiting the formation of tumorspheres and reducing the percentage of $CD44^+$ cells in prostate cancer cells.

Discussion

Since CICs are considered the seed cells for prostate cancer, their eradication may assist in achieving improved results in cancer therapy. CD44 antigen is one of the most important markers for CICs, therefore, the present study constructed salinomycin-encapsulated lipid-PLGA nanoparticles linked with CD44 antibodies, referred to as SM-LPN-CD44. It was identified that SM-LPN-CD44 treatment resulted insignificantly improved potency against CICs compared with free salinomycin treatment or administration of non-targeted nanoparticles.

Unlike biodegradable organic nanoparticles, inorganic nanoparticles cannot be degraded and may therefore cause damage to humans (28,29). These safety considerations significantly limit the potential clinical uses of inorganic nanoparticles (28). By contrast, biodegradable organic nanoparticles provide more promise for clinical application due to their improved safety (28,29). In the present study, the constituent components of SM-LPN-CD44 were PLGA, phosphatidylcholine and cholesterol, all of which are FDA-approved (29). With respect to salinomycin, its therapeutic effects and its potential side effects have been examined in a pilot clinical trial involving patients with cancer, and the results demonstrated that salinomycin administered to the patients exhibited therapeutically beneficial effects and caused no severe side effects (12). In the present study, the results of the CCK-8 assay revealed that blank lipid-PLGA nanoparticles linked with CD44 antibodies were highly biocompatible with prostate cancer cells. Therefore, preliminary safety data from the current study have demonstrated that nanoparticles represent a safe drug delivery system.

Although salinomycin has been demonstrated to exert potent activity against various types of cancer (10-13), to the best of our knowledge, no previous studies have investigated its therapeutic efficacy against $CD44^+$ prostate CICs. The present study revealed that salinomycin preferentially killed $CD44^+$ prostate cancer cells. By performing a cytotoxicity assay, it was identified that the IC_{50} value of SM-LPN-CD44 in $CD44^+$ prostate cancer cells was significantly lower compared with that in $CD44^-$ cells. Using a tumorsphere formation assay, salinomycin was revealed to inhibit the number of tumorspheres propagated in DU145 and 22RV1 passages. Consistent with these findings, it was also demonstrated that the percentage of $CD44^+$ cells in DU145 and 22RV1 cell cultures decreased significantly following salinomycin treatment. To the best of our knowledge, this is the first report that demonstrates the potency of salinomycin against $CD44^+$ prostate CICs.

Antibody-conjugated nanoparticles represent a promising strategy for the treatment of various cancer types, as they can significantly enhance the therapeutic efficacy of chemotherapy drugs (23). Notably, three antibody-conjugated nanoparticles loaded with doxorubicin or docetaxel have previously been successfully translated into early-phase clinical trials (30-32). The results from these trials support the safety and efficacy of antibody-conjugated nanoparticles (30-32). The selection of CD44 antibodies is critical to ensure the specific targeting of the generated nanoparticles to prostate CICs. From the experimental studies it was revealed that in $CD44^+$ prostate CICs, SM-LPN-CD44 demonstrated significantly increased targeting compared with SM-LPN, resulting in increased CIC-specific cytotoxic effects and improved inhibition of tumorsphere formation. However, in $CD44^-$ prostate cancer cells, the cytotoxicity and tumorsphere suppression induced by SM-LPN-CD44 were not significantly greater compared with those induced by SM-LPN. These data firmly demonstrate that SM-LPN-CD44 exhibits improved therapeutic efficacy against prostate CICs, with the linked CD44 antibodies promoting targeting of the nanoparticles to prostate CICs. To the best of our knowledge, the current study is the first to report targeted drug delivery via nanoparticles to prostate CICs through the use of the CD44 antibody.

Since CD44 is a stem cell marker for CICs and hematopoietic stem cells (33), it could be argued that the targeting of SM-LPN-CD44 to CD44 may have potential risks in terms of damage to normal hematopoietic stem cells. However, even in light of this concern, SM-LPN-CD44 is believed to be a promising candidate for further preclinical development for a number of reasons. Firstly, since hematopoietic stem cells and CICs share self-renewal pathways, numerous agents targeting CICs run the risk of damaging hematopoietic stem cells (25). For example, the γ-secretase inhibitors, which have gained attention due to their potential to inhibit Notch signaling, may inhibit CICs and normal stem cells (25). Therefore, a number of CIC-targeting strategies possess the risk of destroying normal hematopoietic stem cells and the problem is not exclusive to our proposed nanoparticles. Furthermore, hematopoietic stem cells exhibit strong regenerative ability and the donation of hematopoietic stem cells can be safely accomplished with the aid of healthy donors (26,27). Therefore, loss of healthy hematopoietic stem cells can easily be treated. Finally, following optimization of the dosing regimen for agents targeting CICs, it is possible that normal stem cells may be found to recover following treatment with a dose that would irreversibly damage the targeted CICs (34).

In conclusion, the present study was the first to report the anticancer activity of salinomycin against prostate CICs, and the first report describing targeted drug delivery via nanoparticles to prostate CICs, using the CD44 antibody. SM-LPN-CD44 nanoparticles were confirmed to selectively target $CD44^+$ prostate CICs. Therefore, these nanoparticles may represent a novel approach towards the treatment of prostate CICs. Since prostate CICs serve a crucial role in drug resistance and metastasis of prostate cancer, patients with a poor prognosis may benefit greatly from the type of targeted therapy proposed and developed in the present study.

Acknowledgements

Not applicable.

Funding

No funding was received.

Availability of data and materials

All data generated or analyzed during this study are included in this published article.

Authors' contributions

YL contributed to the design of the study and wrote the manuscript. JW performed the experiments. JS analyzed the data. All authors have read and approved this manuscript.

Ethics approval and consent to participate

The animal experimental protocols were approved by the Animal Administrative Committee of the Naval Medical University (Shanghai, China).

Patient consent for publication

Not applicable.

Competing interests

The authors declare that they have no competing interests.

References

1. Siegel RL, Miller KD and Jemal A: Cancer statistics, 2017. CA Cancer J Clin 67: 7-30, 2017.
2. Pollock PA, Ludgate A and Wassersug RJ: In 2124, half of all men can count on developing prostate cancer. Curr Oncol 22: 10-12, 2015.
3. Litwin MS and Tan HJ: The diagnosis and treatment of prostate cancer: A review. JAMA 317: 2532-2542, 2017.
4. Sartor O and de Bono JS: Metastatic prostate cancer. N Engl J Med 378: 645-657, 2018.
5. Leão R, Domingos C, Figueiredo A, Hamilton R, Tabori U and Castelo-Branco P: Cancer stem cells in prostate cancer: Implications for targeted therapy. Urol Int 99: 125-136, 2017.
6. Gao J, Li W, Guo Y and Feng SS: Nanomedicine strategies for sustained, controlled and targeted treatment of cancer stem cells. Nanomedicine (Lond) 11: 3261-3282, 2016.
7. Gao J, Feng SS and Guo Y: Nanomedicine for treatment of cancer stem cells. Nanomedicine (Lond) 9: 181-184, 2014.
8. Maitland NJ and Collins AT: Prostate cancer stem cells: A new target for therapy. J Clin Oncol 26: 2862-2870, 2008.
9. Patrawala L, Calhoun T, Schneider-Broussard R, Li H, Bhatia B, Tang S, Reilly JG, Chandra D, Zhou J, Claypool K, *et al*: Highly purified CD44+ prostate cancer cells from xenograft human tumors are enriched in tumorigenic and metastatic progenitor cells. Oncogene 25: 1696-1708, 2006.
10. Gong Z, Chen D, Xie F, Liu J, Zhang H, Zou H, Yu Y, Chen Y, Sun Z, Wang X, *et al*: Codelivery of salinomycin and doxorubicin using nanoliposomes for targeting both liver cancer cells and cancer stem cells. Nanomedicine (Lond) 11: 2565-2579, 2016.
11. Xie F, Zhang S, Liu J, Gong Z, Yang K, Zhang H, Lu Y, Zou H, Yu Y, Chen Y, *et al*: Codelivery of salinomycin and chloroquine by liposomes enables synergistic antitumor activity in vitro. Nanomedicine (Lond) 11: 1831-1846, 2016.
12. Naujokat C and Steinhart R: Salinomycin as a drug for targeting human cancer stem cells. J Biomed Biotechnol 2012: 950658, 2012.
13. Zhang Y, Liu L, Li F, Wu T, Jiang H, Jiang X, Du X and Wang Y: Salinomycin exerts anticancer effects on PC-3 cells and PC-3-derived cancer stem cells in vitro and in vivo. Biomed Res Int 2017: 4101653, 2017.
14. Kim KY, Park KI, Kim SH, Yu SN, Park SG, Kim YW, Seo YK, Ma JY and Ahn SC: Inhibition of autophagy promotes salinomycin-induced apoptosis via reactive oxygen species-mediated PI3K/AKT/mTOR and ERK/p38 MAPK-dependent signaling in human prostate cancer cells. Int J Mol Sci 18: pii: E1088, 2017.
15. Hanrahan K, O'Neill A, Prencipe M, Bugler J, Murphy L, Fabre A, Puhr M, Culig Z, Murphy K and Watson RW: The role of epithelial-mesenchymal transition drivers ZEB1 and ZEB2 in mediating docetaxel-resistant prostate cancer. Mol Oncol 11: 251-265, 2017.
16. Mirkheshti N, Park S, Jiang S, Cropper J, Werner SL, Song CS and Chatterjee B: Dual targeting of androgen receptor and mTORC1 by salinomycin in prostate cancer. Oncotarget 7: 62240-62254, 2016.
17. Wang M, Xie F, Wen X, Chen H, Zhang H, Liu J, Zhang H, Zou H, Yu Y, Chen Y, *et al*: Therapeutic PEG-ceramide nanomicelles synergize with salinomycin to target both liver cancer cells and cancer stem cells. Nanomedicine (Lond) 12: 1025-1042, 2017.
18. Gao J, Xia Y, Chen H, Yu Y, Song J, Li W, Qian W, Wang H, Dai J and Guo Y: Polymer-lipid hybrid nanoparticles conjugated with anti-EGF receptor antibody for targeted drug delivery to hepatocellular carcinoma. Nanomedicine (Lond) 9: 279-293, 2014.
19. Wong HL, Rauth AM, Bendayan R, Manias JL, Ramaswamy M, Liu Z, Erhan SZ and Wu XY: A new polymer-lipid hybrid nanoparticle system increases cytotoxicity of doxorubicin against multidrug-resistant human breast cancer cells. Pharm Res 23: 1574-1585, 2006.
20. Gao J, Chen H, Song H, Su X, Niu F, Li W, Li B, Dai J, Wang H and Guo Y: Antibody-targeted immunoliposomes for cancer treatment. Mini Rev Med Chem 13: 2026-2035, 2013.
21. Guo X, Zhu X, Gao J, Liu D, Dong C and Jin X: PLGA nanoparticles with CD133 aptamers for targeted delivery and sustained release of propranolol to hemangioma. Nanomedicine (Lond) 12: 2611-2624, 2017.
22. Kapoor DN, Bhatia A, Kaur R, Sharma R, Kaur G and Dhawan S: PLGA: A unique polymer for drug delivery. Ther Deliv 6: 41-58, 2015.
23. Gao J, Feng SS and Guo Y: Antibody engineering promotes nanomedicine for cancer treatment. Nanomedicine (Lond) 5: 1141-1145, 2010.
24. Wang J, Wu Z, Pan G, Ni J, Xie F, Jiang B, Wei L, Gao J and Zhou W: Enhanced doxorubicin delivery to hepatocellular carcinoma cells via CD147 antibody-conjugated immunoliposomes. Nanomedicine 16: 1949-1961, 2018.
25. Zhou BB, Zhang H, Damelin M, Geles KG, Grindley JC and Dirks PB: Tumour-initiating cells: Challenges and opportunities for anticancer drug discovery. Nat Rev Drug Discov 8: 806-823, 2009.
26. Chen SH, Wang TF and Yang KL: Hematopoietic stem cell donation. Int J Hematol 97: 446-455, 2013.
27. Billen A, Madrigal JA and Shaw BE: A review of the haematopoietic stem cell donation experience: Is there room for improvement? Bone Marrow Transplant 49: 729-736, 2014.
28. Auffan M, Rose J, Bottero JY, Lowry GV, Jolivet JP and Wiesner MR: Towards a definition of inorganic nanoparticles from an environmental, health and safety perspective. Nat Nanotechnol 4: 634-641, 2009.
29. Cushing BL, Kolesnichenko VL and O'Connor CJ: Recent advances in the liquid-phase syntheses of inorganic nanoparticles. Chem Rev 104: 3893-3946, 2004.
30. Mamot C, Ritschard R, Wicki A, Stehle G, Dieterle T, Bubendorf L, Hilker C, Deuster S, Herrmann R and Rochlitz C: Tolerability, safety, pharmacokinetics, and efficacy of doxorubicin-loaded anti-EGFR immunoliposomes in advanced solid tumours: A phase 1 dose-escalation study. Lancet Oncol 13: 1234-1241, 2012.
31. Miller K, Cortes J, Hurvitz SA, Krop IE, Tripathy D, Verma S, Riahi K, Reynolds JG, Wickham TJ, Molnar I and Yardley DA: HERMIONE: A randomized Phase 2 trial of MM-302 plus trastuzumab versus chemotherapy of physician's choice plus trastuzumab in patients with previously treated, anthracycline-naïve, HER2-positive, locally advanced/metastatic breast cancer. BMC Cancer 16: 352, 2016.
32. Hrkach J, Von Hoff D, Mukkaram Ali M, Andrianova E, Auer J, Campbell T, De Witt D, Figa M, Figueiredo M, Horhota A, *et al*: Preclinical development and clinical translation of a PSMA-targeted docetaxel nanoparticle with a differentiated pharmacological profile. Sci Transl Med 4: 128ra39, 2012.
33. Cao H, Heazlewood SY, Williams B, Cardozo D, Nigro J, Oteiza A and Nilsson SK: The role of CD44 in fetal and adult hematopoietic stem cell regulation. Haematologica 101: 26-37, 2016.
34. Cullion K, Draheim KM, Hermance N, Tammam J, Sharma VM, Ware C, Nikov G, Krishnamoorthy V, Majumder PK and Kelliher MA: Targeting the Notch1 and mTOR pathways in a mouse T-ALL model. Blood 113: 6172-6181, 2009.